

## DIMENSIONALITY OF $\text{CoFe}_2\text{O}_4/\text{LA/SDS-Na/H}_2\text{O}$ FERROFLUID SAMPLE WITH DIFFERENT DILUTION FROM SANS - CURVES MODELLING

Maria BĂLĂȘOIU<sup>1</sup>, Daniela BUZATU<sup>2</sup>, Alexander IVANKOV<sup>3</sup>, Alexandra-Maria BĂLĂȘOIU-GĂINĂ<sup>4</sup>, Sergei LYSENKO<sup>5</sup>, Svetlana ASTAF'EVA<sup>6</sup> and Cristina STAN<sup>7</sup>

*Small-angle neutron scattering (SANS) experimental curves for  $\text{CoFe}_2\text{O}_4/\text{LA/SDS-Na/H}_2\text{O}$  ferrofluid sample with different dilution have been analyzed and modelled using SASView program. The radius of gyration, the mean particle dimension, and Porod exponent are computed for different values of particle volume concentration in the range 1-0.04% at two different temperatures. Dilution effects on the dimensionality of  $\text{CoFe}_2\text{O}_4/\text{LA/SDS-Na/H}_2\text{O}$  ferrofluid ample are detected.*

**Keywords:** SANS curves,  $\text{CoFe}_2\text{O}_4/\text{LA/SDS-Na/H}_2\text{O}$  ferrofluid, Porod coefficient, gyration radius.

### 1. Introduction

In the last few decades, ferrofluid nanoparticles attracted the interest of a large scientific community, due to their special properties based mainly on the low dimensionality and superparamagnetic properties that opens new possibilities for nanotechnology engineering, biosensing and nanomedicine, environmental

<sup>1</sup>PhD, Frank Laboratory of Neutron Physics, Joint Institute of Nuclear Research, Dubna, Russia, National Institute for Physics and Nuclear Engineering, Magurele, Romania; Moscow Institute of Physics and Technology, Dolgoprudny, Russia, e-mail: balas@jinr.ru

<sup>2</sup>Prof., Dept. of Physics, University POLITEHNICA of Bucharest, Romania, e-mail: daniela.buzatu@upb.ro

<sup>3</sup>PhD, Frank Laboratory of Neutron Physics, Joint Institute of Nuclear Research, Dubna, Russia, Moscow Institute of Physics and Technology, Dolgoprudny, Russia; Institute for Safety Problems of Nuclear Power Plants, NAS of Ukraine, 07270 Kyiv, Ukraine, e-mail: ivankov@jinr.ru

<sup>4</sup>Ms., Frank Laboratory of Neutron Physics, Joint Institute of Nuclear Research, Dubna, Russia; West University of Timisoara, Timisoara, Romania; CMCF, Moscow State University, Moscow, Russia, e-mail: alexandra@balasoiu.com

<sup>5</sup>PhD, Institute of Technical Chemistry, Perm Federal Research Center, Ural Branch, Russian Academy of Sciences, Perm, Russia, e-mail: ya.lysenko45@yandex.ru

<sup>6</sup>PhD, Institute of Technical Chemistry, Perm Federal Research Center, Ural Branch, Russian Academy of Sciences, Perm, Russia, e-mail: svetlana-astafeva@yandex.ru

<sup>7</sup>Prof., Dept. of Physics, University POLITEHNICA of Bucharest, Romania, e-mail: cristina.stan@upb.ro

protection and not only [1, 2]. Among possible magnetic fluid nanocomposites, relatively easily to be synthesized, cobalt ferrite nanoparticles are extensively used for their controllable physical and chemical properties that can be tailored for biological and biomedical use [3, 4]. Studies on the stability of the properties of magnetic nanoparticles suspensions and also for of their toxicity and fate in the environment and are also reported [5-7].

Small-angle neutron scattering (SANS) investigation is a powerful technique for obtaining valuable information related to the dimensionality and morphology of the colloidal particle samples and consequently on the modification of these properties at different volume concentration of nanoparticles and temperature variation [8, 9].

## 1. Experimental data

Using the small-angle neutron scattering (SANS) experimental study on different concentrations samples of  $\text{CoFe}_2\text{O}_4/\text{LA/SDS-Na/H}_2\text{O}$  ferrofluid have been performed. The ferrofluid was prepared from  $\text{CoFe}_2\text{O}_4$  nanoparticles obtained by coprecipitation of  $\text{Fe(OH)}_3$  and  $\text{Co(OH)}_2$  and stabilization by the adsorption of lauric acid (LA) on ferrite particles followed by peptisation of hydrophobic precipitate in aqueous solution with sodium n-dodecyl sulphate (SDS) at the Institute of Technical Chemistry, Perm [10, 11].

SANS measurements were performed on the time-of-flight spectrometer with two detector modes [12, 13] in function at the IBR-2 high flux pulsed reactor (JINR Dubna). The SONIX+ software system accomplished the control of the spectrometer [15]. The experiments were carried out at a sample-to-detector distances of 4.5 m and 13 m, resulting in a scattering vector (Q) range of  $0.006\div0.6 \text{ \AA}^{-1}$ .

The scattering intensities (Fig.1) were recorded from ferrofluid samples with the following volume particle concentrations: 1%, 0.5%, 0.25%, 0.16%, 0.07%, 0.04%, as function of the scattering wavevector,  $Q=4\pi \sin 2\theta/\lambda$ , where  $2\theta$  is the scattering angle and  $\lambda$  is the neutron associated wavelength.

For characterizing the sample structure, the most used approximations in small-angle scattering are:

(a) the Guinier approximation for small values of scattering vector [15]

$$I(Q) = Ae^{-\frac{Q^2 R_g^2}{3}} \text{ for } QR_g < 1.3 \quad (1)$$

where  $R_g$  is the radius of gyration and  $A$  is a calibration parameter. The radius of gyration is the second moment of the spatial distribution function of the particle around the center of its scattering.

(b) the power-law approximation [16]

$$I(Q) = \frac{B}{Q^m} \quad \text{for} \quad Q\xi \gg 1 \quad (2)$$

where  $\xi$  is a length that characterizes the size of the structure producing the scattering and  $B$  is a scale constant.

For the experimental data processing the SASView program was used. For the best fit in the Q region,  $0.006 \leq Q \leq 0.07$ , the following functional form was chosen [17]:

$$I(Q) = \begin{cases} \frac{G}{Q^s} \exp\left[\frac{-Q^2 R_g^2}{3-s}\right] & Q \leq Q_1 \\ \frac{D}{Q^m} & Q \geq Q_1 \end{cases} \quad (3)$$

The first branch of  $I(Q)$  according to the above proposed relation (3) represents the generalized Guinier law, where  $s$  is a nondimensional parameter that characterizes the shape of the scattering objects ( $s = 1$  for rods,  $s = 2$  for plates), used as scale constant and:

$$Q_1 = \frac{1}{R_g} \sqrt{(m-s)(3-s)/2}. \quad (4)$$

The second branch describes a power law dependence characteristic to the self-affine structure in the form of mass fractals or of surface fractals. In the case of mass fractal, the fractal dimension varies between 2 and 3 and is equivalent to the Porod exponent. For the surface fractals the fractal dimension is higher than 3 [18, 19].

In Figures 1(a), 2 and 3 the recorded SANS curves at 22 °C, 43 °C and back to 22 °C temperatures are given. In Fig.1 (b) the resulted SANS model curves for different particle concentration for each of the corresponding experimental data set for the temperature 22° C are depicted.

The radius of gyration for a spherical particle is  $R_g^2 = \frac{3}{5}R^2$  [20] and respectively the radius of the particle in the real space is obtained as:  $R_p = R_g \sqrt{\frac{5}{3}}$ .

For processing the SANS data, we choose the cases  $s=0$  for spherical objects.

From the SANS model curves we have extracted the following parameters: radius of gyration ( $R_g$ ) and Porod exponent ( $m$ ) for different values of volume particles concentration.

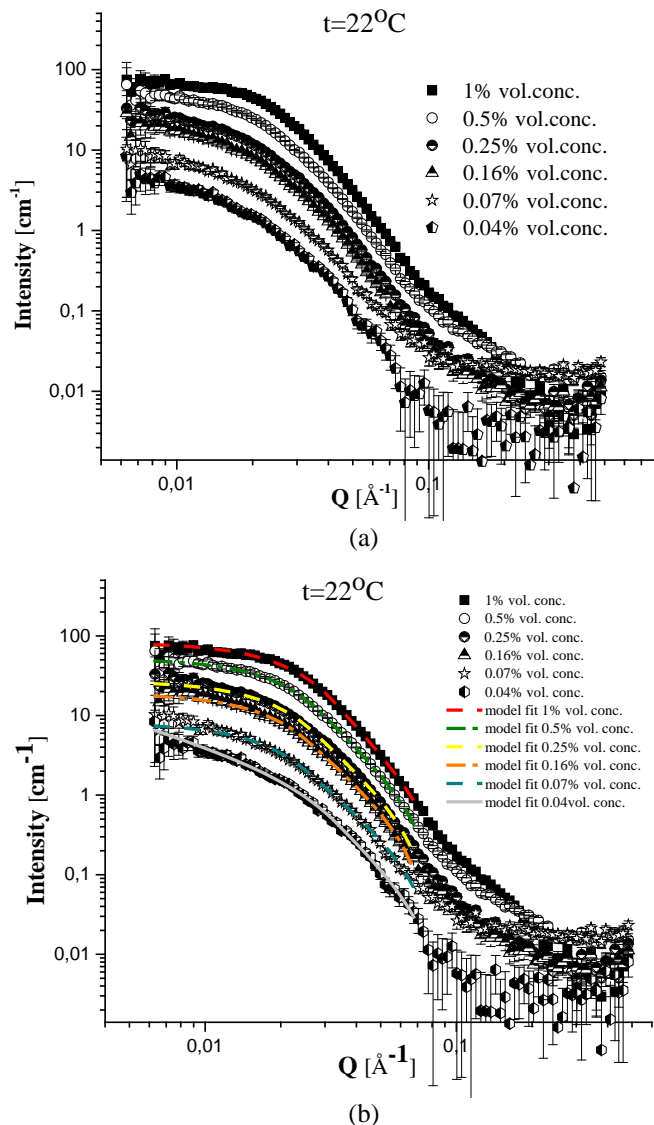


Fig.1. SANS experimental curves for 1%, 0.5%, 0.25%, 0.16%, 0.07% and 0.04% particle vol. concentration of  $\text{CoFe}_2\text{O}_4/\text{LA}/\text{SDS-Na}/\text{H}_2\text{O}$  ferrofluid sample SANS for  $t=22^{\circ}\text{C}$  (a); experimental data and model curves (b).

The computed values of the parameters of interest extracted from the simulated curves for each temperature are given in Tables 1, 2, and 3, respectively.

*Table 1*  
**Values for radius of gyration ( $R_g$ ), radius of particle ( $R_p$ ), Porodexponent ( $m$ )  
for all the sample concentrations in the case  $S = 0$  and  $t=22^\circ\text{C}$ .**

Concentration [vol. %]	Radius of gyration $R_g$ [Å]	Radius of particle $R_p$ [Å]	Porod exponent $m$
1	69.3±0.2	89.4±0.25	3.4
0.5	74.2±0.6	95.7±0.77	3.00
0.25	77.1±0.3	99.5±0.38	2.8
0.16	78.5±0.7	101.3±0.9	2.68
0.07	79.9±1.0	103.1±1.29	2.56
0.04	84.2±2.0	108.6±2.58	2.4

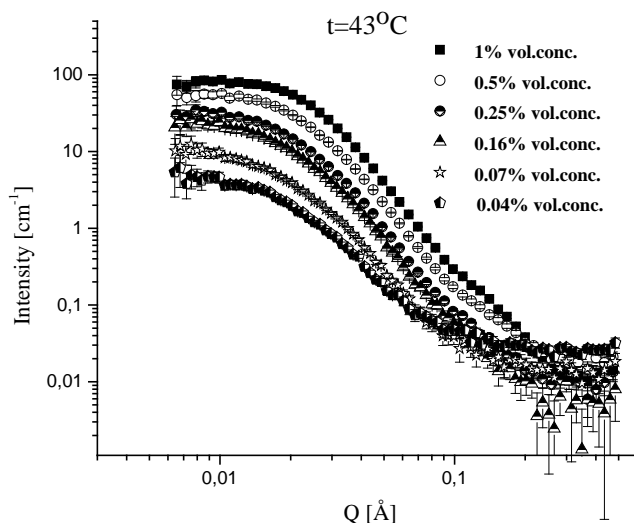


Fig.2 SANS experimental curves for 1%, 0.5%, 0.25%, 0.16%, 0.07% and 0.04% particle vol. concentration of CoFe<sub>2</sub>O<sub>4</sub>/LA/SDS-Na/H<sub>2</sub>O ferrofluid sample at  $t=43^\circ\text{C}$ .

*Table 2*  
**Values for radius of gyration ( $R_g$ ), radius of particle ( $R_p$ ), Porodexponent ( $m$ )  
for all the sample concentrations in the case  $S = 0$  and  $t=43^\circ\text{C}$ .**

Concentration [vol. %]	Radius of gyration $R_g$ [Å]	Radius of particle $R_p$ [Å]	Porod exponent $m$
1	69.0±0.2	89.0 ±0.25	3.43
0.5	73.9±0.4	95.4±0.51	3.10
0.25	77.7±0.5	100.3±0.64	2.89
0.16	79.6±0.7	102.7±0.91	2.71
0.07	83.6±1.3	107.9±1.76	2.47
0.04	81.6±1.8	105.3±2.32	2.37

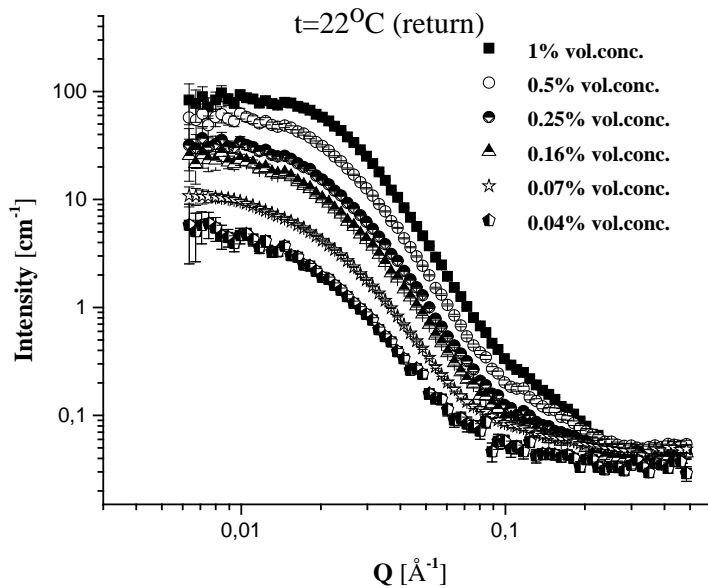


Fig.3 SANS experimental curves for 1%, 0.5%, 0.25%, 0.16%, 0.07% and 0.04% particle vol. concentration of  $\text{CoFe}_2\text{O}_4/\text{LA}/\text{SDS}/\text{H}_2\text{O}$  ferrofluid sample at returning to  $22^\circ\text{C}$ .

*Table 3*  
**Values for radius of gyration ( $R_g$ ), radius of particle ( $R_p$ ), Porod exponent ( $m$ ) for all the sample concentrations returning to  $22^\circ\text{C}$  temperature.**

Concentration [vol. %]	Radius of gyration $R_g$ [Å]	Radius of particle $R_p$ [Å]	Porod exponent $m$
1	$69.7 \pm 0.2$	$89.9 \pm 0.25$	3.4
0.5	$74.7 \pm 0.4$	$96.4 \pm 0.51$	3.07
0.25	$77.7 \pm 0.5$	$100.3 \pm 0.64$	2.84
0.16	$78.5 \pm 0.7$	$101.3 \pm 0.9$	2.75
0.07	$78.8 \pm 0.4$	$101.7 \pm 0.51$	2.47
0.04	$82.1 \pm 1.8$	$105.9 \pm 2.32$	2.43

The plot of the dependence of the gyration radius versus concentration for the analyzed SANS curves are shown in Fig. 4.

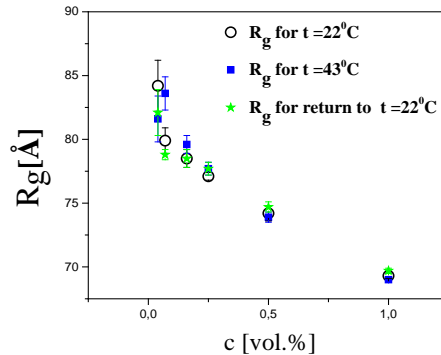


Fig4. Dependence of radii of gyration  $R_g$  versus the particle concentration for  $t=22^\circ\text{C}$ ,  $t=43^\circ\text{C}$  and for returning temperature  $t=22^\circ\text{C}$ .

As clearly seen, in all the cases from Fig. 4, the graphical representations reveal the same typical nonlinear dependences of the gyration radius versus concentration. It abruptly decreases for high dilution and it is followed by an almost linear variation as the particle concentration increases. Consequently, the gyration radius can be considered as a good descriptor for differentiating the effect of the increasing concentration in each sample spatial arrangement.

Plot of the Porod exponents versus particles concentration show an opposite dependence than the gyration radius. As can be observed from Fig. 5, there is a stronger increase for the samples with small dilution and then an almost linear dependence for higher concentration. At higher temperature ( $43^\circ\text{C}$ ) the values of Porod exponents are systematically larger than for  $22^\circ\text{C}$  and returns, excepting for the case of high dilution. As expected, the points corresponding to the return of  $22^\circ\text{C}$  are placed in between the two cases.

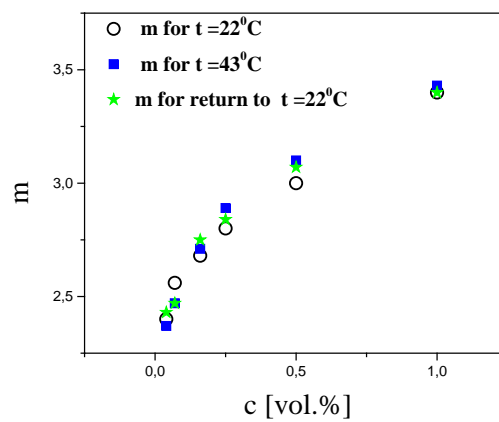


Fig5. Dependence of the Porod exponent  $m$  with the particle concentration for  $t=22^\circ\text{C}$ ,  $t=43^\circ\text{C}$  and for returning temperature  $t=22^\circ\text{C}$ .

An increasing in the Porod exponents also suggests the possibility of aggregation of particles in conglomerates, which are more probable to be generated in an environment with small dilution.

## 6. Conclusions

SANS curves analysis and modelling of the concentration effects on the CoFe<sub>2</sub>O<sub>4</sub>/LA/SDS-Na/H<sub>2</sub>O ferrofluid system have been performed. It is also analyzed the structural effect of temperature variation from t=22°C to t=43°C and return to 22°C.

In the simulation of the experimental curves, a spherical particle approximation is considered. The radii of gyration have been determined in each situation. The values of the radius of gyration increases with decreasing the particle concentration, while the Porod exponents have an opposite variation. It increases as the particles concentration increases, in a specific nonlinear dependence.

The increase in the Porod exponents following the increase of the particle concentration is noted for each temperature. Higher values for the high temperature can be explained as a consequence of the aggregation of some particles. In each case, the Porod coefficient gives a measure of the fractal properties characteristic for specific particle agglomeration behavior.

## Acknowledgements

The authors acknowledge the support from the JINR-Romania projects No. 268 items 14, 31 and No. 269 items 17, 34 (JINR Themes No. 02-2-1124-2015/2020 and No. 04-4-1121-2015/2020).

This work benefited from the use of the SasView application, originally developed under NSF award DMR-0520547. SasView contains code developed with funding from the European Union's Horizon 2020 Research and Innovation Programme under the SINE2020 project, Grant Agreement No. 654000.

## R E F E R E N C E S

- [1] *M. Colombo, S. Carregal-Romero, M. F. Casula, L. Gutiérrez, M. P. Morales, I. B. Böhm, J. T. Heverhagen, D. Prosperi and W.J. Parak*, Biological Applications of Magnetic Nanoparticles, *Chem. Soc. Rev.*, vol. 41, 2012, pp. 4306–4334
- [2] *J. Aswathy and S. Mathew*, Ferrofluids: Synthetic Strategies, Stabilization, Physicochemical Features, Characterization, And Applications, *ChemPlusChem*, vol. 79, 2014, pp. 1382-1420 and the references therein

[3] *E. Fantechi, C. Innocenti, M. Zanardelli, M. Fittipaldi, E. Falvo, M. Carbo, V. Shullani, L. D.C. Mannelli, C. Ghelardini, A. M. Ferretti, A. Ponti, C. Sangregorio, and P. Ceci*, A Smart Platform for Hyperthermia Application in Cancer Treatment: Cobalt-Doped Ferrite Nanoparticles Mineralized in Human Ferritin Cages, *ACS Nano*, Vol 8 (5), 2014, pp.4705-4719

[4] *G. Tiriba, M. Balasoiu, E. Puscasu, L. Sacarescu, C. Stan, D.E. Creanga*, Microstructural characterization of Co-doped iron oxide nanoparticles, *University Politehnica of Bucharest Scientific Bulletin-Series A-Applied Mathematics and Physics*, 79(4), 2017, 327-336.

[5] *L. Popescu, D. Buzatu, M. Balasoiu, C. Stan, B. S. Vasile, L. Sacarescu, D. Creanga, O. Ivankov, D. Soloviov, and A. M. Balasoiu-Gaina*, Study on ageing of cobalt ferrite Nanoparticles and their fate in the environment, *Romanian Journal of Physics* 64 (2019): 818.

[6] *Farooq Ahmad and Ying Zhou*, Pitfalls and Challenges in Nanotoxicology: A Case of Cobalt Ferrite (CoFe<sub>2</sub>O<sub>4</sub>) Nanocomposites *Chemical Research in Toxicology* 2017 30 (2), 492-507

[7] *I. Bodale, M. Oprisan, C. Stan, F. Tufescu, M. Racuciu, D. Creanga, and M. Balasoiu*, Nanotechnological Application Based on CoFe<sub>2</sub>O<sub>4</sub>, "Nanoparticles and Electromagnetic Exposure on Agrotechnical Plant Growth in: Sontea V., Tiginyanu I. (eds) 3rd International Conference on Nanotechnologies and Biomedical Engineering. IFMBE Proceedings, Springer, Singapore, vol. 55, 2016, pp 153-156

[8] *M. Avdeev, M. Balasoiu, Gy. Tork, D. Bica, L. Rosta, V.L. Aksenov, L. Vekas*, SANS study of particle concentration influence on ferrofluid nanostructure, *Journal of Magnetism and Magnetic Materials* 252 (2002) 86–88

[9] *A.-M. Balasoiu-Gaina, M. Balasoiu, O. Ivankov, D. Soloviov, S. Lysenko, C. Stan, N. Lupu, D. Creanga, and A. Kuklin*, Structural analysis of aqueous ferrofluids with cobalt ferrite particles stabilized with lauric acid and sodium n-dodecyl sulphate, *J. Phys. Conf. Ser.*, vol. 848 (2017) 12026

[10] *S. N. Lysenko, A. V. Lebedev, S. A. Astaf'eva, D. E. Yakusheva, M. Balasoiu, A. I. Kuklin, Yu. S. Kovalev, V. A. Turchenko*, Preparation and magneto-optical behavior of ferrofluids with anisometric particles, *Physica Scripta* 95 (2020) 044007

[11] *M. Balasoiu, O. I. Ivankov, D.V. Soloviov, S.N. Lysenko, R.M. Yakushev, A.-M. Balasoiu-Gaina, N. Lupu*, Microstructure investigation of a CoFe<sub>2</sub>O<sub>4</sub>/lauric acid/DDS-Na/H<sub>2</sub>O ferrofluid, *Journal of Optoelectronics and advanced Materials* 17(7-8) (2015) 1114 – 1121.

[12] *A.I. Kuklin, A.I. Ivankov, D.V. Soloviov, A.V. Rogachev, Yu.S. Kovalev, A.G. Soloviev, A.Kh. Islamov, M. Bălașoiu, A.V. Vlasov, S.A. Kutuzov, A.P. Sirotin, A.S. Kirilov, V.V. Skoi, M.I. Rulev and V.I. Gordeliy*, High-throughput SANS experiment on two-detector system of YuMO spectrometer, *J. Phys. Conf. Ser.*, 994 (2018) 1-7

[13] *A.G. Soloviev, T.M. Solovjeva, O.I. Ivankov, D.V. Soloviev, A.V. Rogachev, A.I. Kuklin*, SAS program for two-detector system: seamless curve from both detectors, *J. Phys.: Conf. Ser.* 848 (2017) 012020

[14] *A.S. Kirilov, E.I. Litvinenko, N.V. Astakhova, S.M. Murashkevich, T.B. Petukhova, V.E. Yudin, V.I. Gordelii, A.Kh. Islamov, A.I. Kuklin*, Evolution of the SONIX software package for the YuMO spectrometer at the IBR-2 reactor, *Instrum. Exp. Tech.*, 47(3) (2004) 334-345 DOI:<https://doi.org/10.1023/B:INET.0000032899.51622.1e>

[15] *A. Guinier & G. Fournet*, Small-Angle Scattering of X-rays. New York: Wiley (1955)

[16] *G. Porod*, Small-Angle X-ray Scattering, edited by O. Glatter & O. Kratky. pp. 17–51. London: Academic Press (1982)

[17] *B. Hammouda*, A new Guinier-Porod model, *Journal of Applied Crystallography* 43 (2010) 716-719

[18] *C. Stan, M. Balasoiu, D. Buzatu, C.P. Cristescu*, Multifractal Analysis of CoFe<sub>2</sub>O<sub>4</sub>/Lauric Acid/DDS-Na/H<sub>2</sub>O Ferrofluid from Transmission Electron Microscopy Measurements, *Journal of Computational and Theoretical Nanoscience*, 14(4), (2017) 2030-2034.

- [19] *C. Stan, M. Balasoiu, A. Ivankov, C.P. Cristescu*, Multifractal analysis of CoFe<sub>2</sub>O<sub>4</sub>/2DBS/H<sub>2</sub>O ferrofluid from tem and sans measurements, *Romanian Reports in Physics*, 68(1), (2016) 270-277.
- [20] *L.A. Feigin and D.I. Svergun*, *Structure Analysis by Small-Angle X-Ray and Neutron Scattering*, Plenum Press, New York (1987)